2014

High-Efficiency Thrust Vector Control Allocation

Jeb S. Orr

Nathan Slegers
George Fox University, nslegers@georgefox.edu

High-Efficiency Thrust Vector Control Allocation

Jeb S. Orr*
The Charles Stark Draper Laboratory, Inc., Huntsville, Alabama 35812
and
Nathan J. Slegers†
University of Alabama in Huntsville, Huntsville, Alabama 35816

A generalized approach to the allocation of redundant thrust vector slew commands for multi-actuated launch vehicles is presented, where deflection constraints are expressed as omniaxial or elliptical deflection limits in gimbal axes. More importantly than in the aircraft control allocation problem, linear allocators (pseudoinverses) are preferred for large booster applications to facilitate accurate prediction of the control-structure interaction resulting from thrust vectoring effects. However, strictly linear transformations for the allocation of redundant controls cannot, in general, access all of the attainable moments for which there is a set of control effector positions that satisfies the constraints. In this paper, the control allocation efficiency of a certain class of linear allocators subject to multiple quadratic constraints is analyzed, and a novel single-pass control allocation scheme is proposed that augments the pseudoinverse near the boundary of the attainable set. The controls are determined over a substantial volume of the attainable set using only a linear transformation; as such, the algorithm maintains compatibility with frequency-domain approaches to the analysis of the vehicle closed-loop elastic stability. Numerical results using a model of a winged reusable booster system illustrate the proposed technique's ability to access a larger fraction of the attainable set than a pseudoinverse alone.

Nomenclature

a_{ij}	=	principal axis lengths of ith constraint ellipsoid, rad
B	=	control effectiveness sensitivity matrix, $1/s^2$
B_i	=	submatrix of B associated with ith engine, $1/s^2$
c_i	=	constraint scaling constant associated with ith engine
F_i	=	thrust force of ith engine, lbf
H	=	scalar cost function
I	=	identity matrix
$\hat{i}_G, \hat{j}_G, \hat{k}_G$	=	orthonormal basis of gimbal frame G
J	=	rigid body moment of inertia tensor, slug $\cdot$ ft^2
k	=	number of engines
l	=	unit vector in $\mathbb{R}^n$
M	=	moment sensitivity matrix, ft $\cdot$ lbf/rad
m	=	number of control inputs; $2k$
N_P	=	matrix with columns forming a basis for kernel of $PB - I$
N_B	=	matrix with columns forming a basis for kernel of B
n	=	number of controlled degrees of freedom
p	=	number of parameters used to determine a generalized inverse P
R	=	null space projecting transformation
r_{Gi}	=	location of ith engine with respect to vehicle center of mass, ft
S	=	inverse allocation weight matrix
T_i^A	=	thrust vector transformation matrix due to actuation
T_i^G	=	transformation of nozzle angular degrees of freedom from gimbal to body
u_i, u_i'	=	null-position and perturbed thrust unit vector, respectively
W	=	allocation weight matrix
Γ	=	perturbation angular acceleration, rad/s^2
Γ_c	=	perturbation angular acceleration, commanded, rad/s^2
γ_i	=	image of thrust deflection δ_i under the transformation B_i
Δ	=	control vector of thrust deflections, rad
$\Delta_0, \Delta_s, \Delta_e$	=	component of control vector within, on, and outside the admissible set, respectively
$\tilde{\Delta}$	=	augmented control vector, rad
δ_i	=	vector in $\mathbb{R}^2$ of small thrust rotations in gimbal frame, rad
$\mathcal{E}_i(R_i)$	=	constraint ellipsoid of ith engine having shape matrix R_i
$\mathcal{E}_i'(Q_i)$	=	image under B of ith engine's constraint ellipsoid having shape matrix Q_i
η	=	allocation efficiency
θ_i	=	vector in $\mathbb{R}^3$ of small thrust rotations in body frame, rad
κ	=	positive scaling constant
λ	=	vector of Lagrange multipliers
ξ_j	=	jth basis vector of kernel of B
$\Phi, \partial(\Phi)$	=	set of achievable angular accelerations and its boundary
$\Phi^\star$	=	particular subset of achievable angular accelerations using a linear inverse
$\Phi^{\star\star}$	=	subset of achievable angular accelerations using a linear inverse and command augmentation
$\Omega, \Omega^\circ, \Omega^e, \partial(\Omega)$	=	set of admissible control deflections and its interior, exterior, and boundary, respectively
$\Omega^\star$	=	subset of controls corresponding to $\Phi^\star$
ω	=	rigid body angular velocity, rad/s

I. Introduction

THE use of optimal control allocation has received extensive attention in the literature, particularly in the context of aircraft control [1,2]. Typically, high-performance aircraft are designed with significantly overlapping control moment effectiveness at a particular flight condition, and so the resultant control allocation solution is underdetermined. Likewise, in the context of launch vehicle

Received 16 January 2013; revision received 22 May 2013; accepted for publication 24 May 2013; published online 5 February 2014.

*Senior Member of the Technical Staff, Dynamics and Control; jorr@draper.com (Corresponding Author).

†Associate Professor, Department of Aerospace Engineering.

dynamics, the proposed development of both heavy-lift rockets and small reusable (flyback) boosters has led to interest in the applications of optimal control allocation schemes to systems with multiple gimbaled rocket nozzles.

Durham [3–5] developed the fundamental theory of the allocation of redundant effectors with constraints and proposed algorithms such as the well-known direct method [6–8] to allocate them. Thereafter, Bordignon [9] extended the theory and evaluated numerous methods for solving the underlying constrained optimization problem. More recently, an interest has developed in considering higher-dimensional objective spaces, such as structural loads [10,11], the supporting theory for which was explored by Beck [12]. In the context of solving the three-moment constrained control allocation problem, much of the existing literature has focused on efficient numerical optimization methods that are practically implementable in the flight software [2,8,13–16], relaxing the requirement that the moments are globally linear in the controls [17,18], explicit consideration of the actuator dynamics [19], and fault tolerance [20,21].

To enhance performance margins, crew safety, and likelihood of mission success, it is desirable to design a control allocation mechanism that is capable of effecting the maximum possible angular accelerations on the vehicle within the capability of the control actuators. However, achieving all feasible control objectives requires the use of an online nonlinear optimization scheme. As a matter of engineering practice in the launch vehicle community, it is preferred that nonlinear behaviors are relegated to the edges of the performance envelope. For example, conservative linear stability analysis techniques are often considered mandatory for human-rated launch systems [22]. Nonlinear behaviors are more easily justified if they improve performance for off-nominal conditions and only affect behavior in what are likely to already be failure scenarios. Notwithstanding the flight certification environment, the application of algorithms with variable convergence characteristics [2] raises concerns about computational feasibility. Finally, some common formulations (such as quadratic programming) are not compatible with nonpolytopic constraint geometries.

Unlike in some aircraft where actuator servoelastic coupling and inertial reaction torques may be ignored under the premise that the control allocation algorithm provides only the required rigid body angular acceleration, these effects are nonnegligible and often dynamically significant for large flexible rocket vehicles with nonminimum-phase parasitic elastic dynamics [23,24]. The use of multiple engines with varied servodynamics requires that the exact combination of actuators to be employed at any flight condition is known; for stability analysis, it is insufficient to assume that the command is automatically achieved by the control allocator in light of the dynamics affecting the motion of applied thrust and the inertial coupling (tail-wag-dog effect) of the relatively heavy engines themselves.

In the case of gimbaled rocket engines, the maximum control deflection is ultimately limited by the linear travel of the actuators, which are often of the high-power hydraulic type. Other constraints may dictate the upper limits on the nozzle slew angle with respect to the null position. These include margins to prevent bell interference or recontact with other stage hardware, flexure limits on propellant and oxidizer feedline ducts, and constraints to mitigate plume impingement or other flow interaction effects. Solely because of the actuator kinematics, the boundary of admissible vectoring angles is not a rectangular constraint. When all limiting factors are considered, a common method of expressing the constraint is as an omniaxial (root-sum-square) limit on the thrust vectoring angle that prescribes a circular boundary. To maximize the generality of the present approach, this circular boundary will be expressed as an ellipse in $\mathbb{R}^2$.

Multi-actuated thrust-vector control systems of this type are common in launch vehicles, and always yield redundant control authority for nondegenerate geometries. If the null positions of the thrust vectors are symmetric with respect to the control axes and nominally aligned along the vehicle symmetry axis, the control mixing required to effect accelerations in roll, pitch, and yaw is trivial and no special algorithm is warranted. However, complex asymmetric geometries with differing thrust levels and constraints do not admit obvious solutions. A control allocation algorithm must be employed to both maximize performance capability and minimize adverse effects such as steering (cosine) losses and internal structural loads.

One particularly challenging problem in the design of control allocators is determining the shape of the set of attainable moments that are achievable using a particular allocation strategy, and comparing it with the extremal set of moments that are theoretically attainable subject to the constraints [4,5]. The former is usually that which can be accessed using a simple online algorithm, and the latter requires an iterative optimization approach that is undesirable for launch vehicle flight software implementation. Although research into the optimal allocation of constrained controls has yielded a rich literature beginning with Durham's seminal paper [3], the existing theory treats only constraints that can be expressed as a linear inequality; that is, independent saturation limits that describe a polytope bounding the admissible controls. There has been virtually no treatment of constraint geometries not expressible as linear inequalities except to approximate them to fit within the existing mathematical framework [13]. As will be shown, the use of multiple quadratic inequality constraints admits the convenient set properties of ellipsoids under linear transformations [25] and the ellipsoidal calculus [26]. This framework can be employed to rapidly ascertain the boundary of the set of attainable moments under relatively general conditions.

Most importantly, the application of a control allocation algorithm to launch vehicles necessitates compatibility of the design paradigm with the heritage flight certification processes that dominate the space access industry. Because of their complexity and nonlinearity, iterative control allocation algorithms used to resolve effector saturation are difficult to reconcile with the present application. Instead, a single-pass null-space augmentation method conceptually analogous to that presented by Bordignon and Durham [27] and JingPing et al. [28] is proposed. As a result of a novel projection technique and the presence of an analytic constraint geometry, it is shown not only to be a computationally feasible algorithm, but a highly effective approach for increasing the control allocator efficiency while maintaining linearity over a substantial portion of the total capability.

The organization of the paper is as follows. The statement of the thrust vector control allocation problem is given in Sec. II. In Sec. III, the geometries of the total and particular sets of attainable moments are derived for a general, multi-actuated thrust vector controlled system subject to elliptical constraints, and the volume metric of allocation efficiency is introduced. The null-space augmentation method for high-efficiency allocation of controls exceeding the capability of a linear allocator is proposed in Sec. IV, along with numerical results in Sec. V that demonstrate the efficacy of the proposed approach as applied to a nontrivial vehicle geometry.

II. Problem Statement

The general control allocation problem is concerned with the mapping of the deflections of m actuators into an n-dimensional moment space, and the relationship of a closed, bounded, and convex set Ω of admissible control deflections in $\mathbb{R}^m$ to its associated closed, bounded, and convex set of achievable moments Φ in $\mathbb{R}^n$. As a matter of numerical and practical convenience, the space Φ is that of angular accelerations in $\mathbb{R}^3$. For consistency with the existing control allocation literature, this will be referred to as a moment space. In this application, the simultaneous control of three angular degrees of freedom of the rigid body are considered. The rigid-body dynamics are given by [24]

$$J\dot{\omega} + \omega^{\times} J\omega = \sum_{i=1}^{k} F_i r_{Gi}^{\times} u_i' \tag{1}$$

where J is the integrated vehicle inertia tensor and $\omega \in \mathbb{R}^3$ are the body angular rates; the notation $(\,)^{\times}$ forms the skew-symmetric cross-product matrix of appropriate size.

Each engine is described by its location r_{Gi} with respect to the center of mass, its thrust F_i, and its instantaneous thrust unit vector u_i', expressed in the body frame. The deflected thrust vector is related to the null position unit vector u_i by a kinematic transformation

$$u_i' = T_i^A u_i \tag{2}$$

The null position is associated with zero actuator deflection, and so T_i^A is nominally the identity matrix. With respect to perturbations, it is assumed that the angular deflections of the nozzle are small and that the nonlinear attitude dynamics can be neglected. The kinematic relationship of the unit null vector can be expanded via skew-symmetric small rotations, and Eq. (1) becomes

$$J(\dot{\omega} - \dot{\omega}_0) = \sum_{i=1}^{k} F_i r_{Gi}^{\times} u_i - \sum_{i=1}^{k} F_i r_{Gi}^{\times} u_i^{\times} \theta_i \tag{3}$$

where $\theta_i \in \mathbb{R}^3$ is a vector of small rotations relating the deflected thrust vector to its null position in the body frame. Without loss of generality, it is assumed that there exists a combination of u_i such that the first terms in the sum on the right-hand side of Eq. (3) are zero; that is, there exists some combination of nominal engine cant angles u_i at each flight condition such that the net moment is zero.

Because each gimbaled nozzle has only two degrees of freedom, let $T_i^G \in \mathbb{R}^{3\times 2}$ be the transformation that maps the nondegenerate local pitch–yaw ("rock" and "tilt") deflections of the nozzle into the body frame, and let these angles be described by a vector pair of local perturbation angles $\delta_i \in \mathbb{R}^2$ about directions normal to the thrust axis.

The geometry of an idealized nozzle is shown in Fig. 1. The G or gimbal frame is defined by a basis $\hat{i}_G, \hat{j}_G, \hat{k}_G$, where $\hat{i}_G$ is aligned with the thrust unit vector at its null position. Generally, $\hat{j}_G$ and $\hat{k}_G$ are chosen to correspond to the axes about which actuator extension or retraction rotates the nozzle; the first and second elements of δ_i correspond to rotation about $\hat{j}_G$ and $\hat{k}_G$, respectively. The use of T_i^G eliminates the redundant degree of freedom associated with rotation of the engine about its thrust axis.

Considering the linear dependence of Eq. (3) on θ_i, the moment sensitivity matrix $M \in \mathbb{R}^{n\times m}$ can be written as

$$M = [-F_1 r_{G1}^{\times} u_1^{\times} T_1^G \quad -F_2 r_{G2}^{\times} u_2^{\times} T_2^G \quad \dots \quad -F_k r_{Gk}^{\times} u_k^{\times} T_k^G] \tag{4}$$

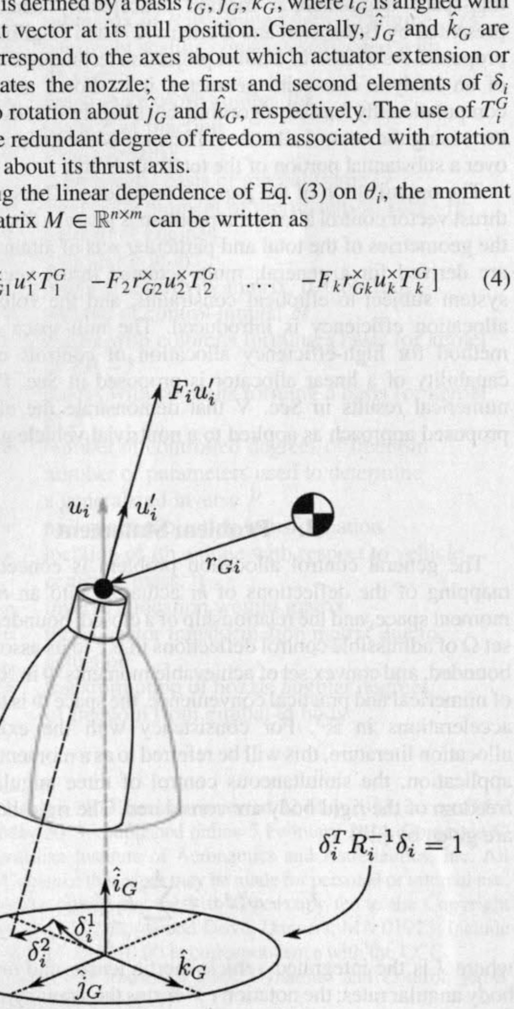

Fig. 1 Thrust vector geometry.

Let the control vector $\Delta \in \mathbb{R}^m$ be given by

$$\Delta = [\delta_1^T \quad \delta_2^T \quad \dots \quad \delta_k^T]^T \tag{5}$$

Under the foregoing assumptions, it follows that

$$\Gamma = B\Delta \tag{6}$$

where the perturbation angular acceleration $\dot{\omega} - \dot{\omega}_0 = \Gamma$ and $B = J^{-1}M$ is the control effectiveness matrix expressed in units of angular acceleration per unit angle of nozzle deflection. In general, B is varying in time as the parameters change due to the consumption of vehicle propellant. It is furthermore assumed that B has column rank n, which is assured for nondegenerate geometries and nonzero thrusts F_i.

By virtue of the kinematic restrictions on the nozzle deflections, let there be associated with each constraint on δ_i the admissible ellipsoid $\mathcal{E}_i(R_i)$ where

$$\mathcal{E}_i(R_i) = \{\delta_i \in \mathbb{R}^2 | \delta_i^T R_i^{-1} \delta_i \leq 1\} \tag{7}$$

and $R_i \in \mathbb{R}^{2\times 2}$ is a symmetric, positive-definite matrix; for example, a circular constraint is the special case where R_i is a scalar multiple of the identity matrix.

Because there exist k independent, symmetric constraints on the control vectors δ_i, the admissible controls lie within a closed and bounded set

$$\Omega = \{\Delta \in \mathbb{R}^m | \delta_i \in \mathcal{E}_i, \quad \forall\ i\} \tag{8}$$

Under the linear transformation B, there exists a compact convex set of attainable moments $\Phi \in \mathbb{R}^n$,

$$\Phi = \{B\Delta \in \mathbb{R}^n | \Delta \in \Omega\} \tag{9}$$

the image of Ω. The set Φ is hereafter referred to as the attainable moment set (AMS).

The general thrust vector control allocation problem is as follows: given an attainable command $\Gamma_c \in \Phi$, one seeks to determine a set of control effector deflections Δ that minimizes some convex metric $H(\Delta)$ subject to the constraints $\Gamma = \Gamma_c$ and $\Delta \in \Omega$. In general, because $\text{rank}(B) = n$ and $m > n$, there may exist multiple Δ that satisfy $\Gamma_c = B\Delta$ if $\Gamma_c \in \Phi$. If the command is infeasible ($\Gamma_c \notin \Phi$), the goal is to generate a response that minimizes some alternative error metric $H'(\Gamma - B\Delta)$ while still satisfying the constraints $\Delta \in \Omega$. The obvious choice of minimizing $\|\Gamma - B\Delta\|_2$ may be undesirable because it can lead to a loss of collinearity between the achieved response and the command. For this reason, infeasible commands can be accommodated via scaling. Solution approaches for infeasible commands are not treated in this paper.

For commands within the attainable set and owing to the aforementioned practical considerations, it is desired that Δ be determined over a substantial volume of Φ using a linear transformation rather than the online solution of a constrained optimization problem. As was shown by Durham [3] in application to the allocation of redundant controls for aircraft, a right generalized inverse P satisfying $BP = I$ can be determined that efficiently allocates redundant controls to satisfy commands Γ_c in some proper subset $\Phi^\star \subset \Phi$ without violating the constraints; that is, a linear control allocation law P cannot access all of Φ. Although the basis of the argument is similar to that given by Durham for aircraft, the underlying topology is markedly different owing to the unique nature of the constraints. The details will be explored in the following section.

III. Determining Φ and $\Phi^\star$ with Elliptical Constraints

In the existing control allocation literature, the set of attainable moments is readily given by the image under B of the m-dimensional polytope Ω, found by determining via binary enumeration the vertices of the m-simplex representing all possible combinations of controls set at their limits [5]. In comparison with coupled analytic constraints on the controls, the geometry of Φ can be determined from the properties of ellipsoids under linear transformations.

Each admissible set in Eq. (7) is an ellipse in $\mathbb{R}^2$ or, equivalently, a degenerate ellipsoid (having $m-2$ degenerate eigenvalues) in the m-dimensional space. Note that each $\mathcal{E}_i$ is wholly contained in a two-dimensional subspace. The admissible controls Ω are found from the union of $\mathcal{E}_i$ in $\mathbb{R}^m$, and the attainable moments are the image of this union Ω under the linear transformation B. The set Ω is a closed, bounded, and convex set in $\mathbb{R}^m$, and its image under B (if B is full rank) is necessarily also closed, bounded, and convex.

Because each δ_i are independent, the $\mathcal{E}_i$ are nonintersecting in $\mathbb{R}^m$ and it follows that Φ can be found via the Minkowski (direct) sum of the images of $\mathcal{E}_i$ under an appropriate partitioning of B. Let the image of $\mathcal{E}_i$ under the blockwise-component transformation of B be given by

$$\mathcal{E}_i'(Q_i) = B_i\mathcal{E}_i = \{\gamma_i \in \mathbb{R}^3 | \gamma_i^T Q_i^{-1}\gamma_i \le 1\} \tag{10}$$

noting that R_i transforms as a rank-2 tensor and

$$Q_i = B_i R_i B_i^T \tag{11}$$

after partitioning B conformably as

$$B = [B_1 \quad B_2 \quad \dots \quad B_k] \tag{12}$$

Assuming each $B_i \in \mathbb{R}^{n\times 2}$ has full column rank, the image of R_i in $\mathbb{R}^n$ is a disk; Q_i is symmetric, positive semidefinite, and always has $n-2$ zero eigenvalues whose eigenvectors are in the kernel of B_i^T (Fig. 2). Thus, the inverse of the positive-semidefinite matrix Q_i is to be interpreted as its generalized inverse in this context.

The set of attainable moments is given by

$$\Phi = B\bigcup \mathcal{E}_i = \mathcal{E}_1' \oplus \mathcal{E}_2' \oplus \dots \oplus \mathcal{E}_k' \ominus B\bigcap \mathcal{E}_i \tag{13}$$

noting, in particular, the intersection in Eq. (13). There exist no general methods to compute the intersection of degenerate hyperellipsoids. In Eq. (13), the intersection is identically zero owing to the disjoint constraints. Thus, the Minkowski sum is computable and the set of attainable moments can be determined.

As was shown in [29], the computation of the Minkowski sum in Eq. (13) can be accomplished using various methods; for example, it can be approximated to arbitrary precision via the use of multiple internal and external approximating ellipsoids along directions $l \in \mathbb{R}^3$ [30]; it can be inscribed with a unique maximum-volume ellipsoid $\mathcal{E}(Q)$, the John ellipsoid [31], or it can be computed numerically [33].

A. Generalized Inverses

Pervasive in the controls literature is the use of right generalized inverses for the allocation of redundant controls; that is, linear transformations that compute solutions to Eq. (6). If B is full rank and $m > n$, there are an infinite number of generalized inverses P that satisfy

$$BP = I \tag{14}$$

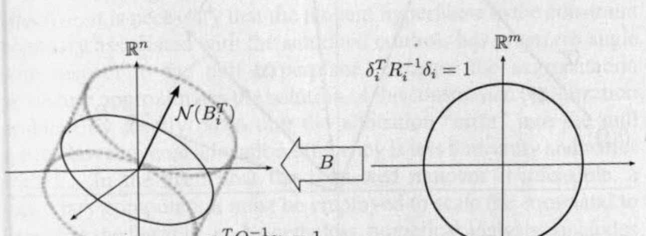

Fig. 2 Image of constraint boundary as a cylinder (disk) in $\mathbb{R}^n$.

In the general case, the number of free parameters in the determination of P is $(m-n)n$ [3]. Let P be parametrized by a vector of size p. If $p < (m-n)n$, the generalized inverse P will be referred to as a structured generalized inverse. Conversely, an inverse for which $p = (m-n)n$ is known as a tailored generalized inverse [9]. Structured inverses arise by imposing constraints on the solution other than Eq. (14), which reduces the number of parameters. The most restrictive generalized inverse is the well-known Moore–Penrose inverse, which satisfies all four Penrose conditions and has the convenient property of producing solutions that lie wholly outside of the null space of B [32]. This important fact will be of interest in a later section.

B. Generalized Inverses and Constraints

Generalized inverse solutions to the control allocation problem are favored due to their linearity, but they do not take into account the limits on the controls. As such, along each unit direction $l \in \mathbb{R}^n$, there exists some positive constant κ such that

$$\kappa Pl \in \partial(\Omega) \tag{15}$$

At least one of the controlled degrees of freedom has intersected the boundary $\partial(\Omega)$ of the set of admissible controls. In general, however, this does not imply that $\kappa BPl \in \partial(\Phi)$ for all l. Under a generalized inverse, only a subset of the admissible controls maps to the boundary of the attainable moment set. This leads to the following theorem:

Theorem 1: Given the linear map $\Gamma = B\Delta$, $\Gamma \in \mathbb{R}^n$, $\Delta \in \mathbb{R}^m$, $m > n$, a compact, convex geometric constraint $\Delta \in \Omega$, and any linear allocator P satisfying $BP = I$, the associated particular AMS $\Phi^\star$ is a proper subset of the total AMS Φ.

Proof: The following proof is similar to that given by Durham [3] and is fundamental in the linear allocation problem. Consider the subset of controls $\Psi = \{\Delta \in \partial(\Omega)\}$ that lie on the boundary $\partial(\Omega)$. Because Ω is bounded, the span of Ψ is m. Suppose that $\Phi^\star = \Phi$. Then, $PB\Delta \in \partial(\Omega)\ \forall\ \Delta \in \Psi$, and so $\Delta = PB\Delta \Rightarrow (PB - I)\Delta = 0$ $\forall\ \Delta \in \Psi$. If this is true, then $\mathrm{span}(\mathcal{N}(PB - I)) = m$. This cannot hold if $m > n$, implying $\Phi^\star \subset \Phi$ by contradiction. □

Geometrically speaking, the attainable moment set under a particular inverse P, introduced earlier as $\Phi^\star$ and referred to as the particular AMS, is a proper subset of the total AMS Φ:

$$\Phi^\star = \{B\Delta | PB\Delta \in \Omega\}$$

Because B is a mapping onto an n-dimensional space, it follows that only some subset of controls Δ map to the boundary of Φ; the remainder map to its interior. The kernel of $PB - I$ spans an n-dimensional subspace of $\mathbb{R}^m$ that contains $\Omega^\star$, the inverse image of $\Phi^\star$ [3]. Let $N_P \in \mathbb{R}^{m\times n}$ be formed from a basis for $\mathcal{N}(PB - I)$. It follows that the orthogonal projection of Ω onto the subspace defined by N_P yields the particular constraint set

$$\Omega^\star = N_P(N_P^T N_P)^{-1} N_P^T \Omega \tag{16}$$

The image of $\Omega^\star$ under B is indeed the elusive particular AMS. However, computation of the projection in Eq. (16) invalidates the prior assumption that the inverse images of R_i have no intersection in $\mathbb{R}^m$. This complication precludes the analytic computation of the particular AMS using Eq. (13). Under certain conditions when intersections do not occur or through approximation methods [29], the particular AMS can be determined using ellipsoidal techniques to some degree of accuracy. However, the requisite linear algebra operations, practically speaking, exceed the computational effort required to determine $\Phi^\star$ directly via a gridded bisection search.

The gridded bisection search method allows for efficient direct computation of the particular AMS. In this method, the unit ball is sampled to yield a set of unit directions l. (Because of symmetry, only one-half of the space must be sampled). For each unique l, $\kappa(l)$ is determined via a bisection method. The convex hull of the resultant point set yields an affine approximation to the particular AMS. Examples appear in Sec. V.

C. Allocation Efficiency

Given a general control allocation scheme $\Delta = f(\Gamma_c)$, the allocation efficiency η is defined as the volume ratio of the attainable set $\Phi^\star$ versus the theoretical upper bound:

$$\eta = \frac{\mathrm{vol}(\Phi^\star)}{\mathrm{vol}(\Phi)} \tag{17}$$

The volume of the total and particular AMS can be computed to a high degree of accuracy using standard convex hull algorithms, or can be approximated using the log determinant of a maximally inscribed ellipsoid, as was shown in [29].

IV. High-Efficiency Quasi-Linear Algorithm

The use of a structured generalized inverse has distinct advantages in the allocation of redundant controls; namely, it is linear, it can be precomputed or easily computed online, and it is deterministic and noniterative. The properly parametrized weighted least squares (WLS) generalized inverse is a convenient structured inverse that minimizes the weighted norm of the control deflection vector and provides better allocation efficiency in many scenarios than the Moore–Penrose inverse.

The WLS inverse minimizes the cost function

$$H(\Delta) = \frac{1}{2}\Delta^T S \Delta + \lambda^T(\Gamma_c - B\Delta) \tag{18}$$

where $S \in \mathbb{R}^{m\times m}$ is a symmetric positive semidefinite matrix and λ is a vector of Lagrange multipliers in the usual sense. Letting the weight matrix $W = S^{-1}$ (or its appropriate pseudo-inverse in the case that W is positive semidefinite), Eq. (18) has a global minimum given by the well-known weighted least squares solution:

$$\Delta = WB^T(BWB^T)^{-1}\Gamma_c \tag{19}$$

If W is in its simplest diagonal form, the requisite computations are sparse and are readily implementable in flight software without substantial computational penalty. The WLS allocator provides high volumetric efficiency for most geometries and, although not as general as the tailored inverse, it does not require optimization to determine the parameters. In addition, the convex cost function in Eq. (18) has a global minimum, whereas the tailored inverse may not [9]. Finally, the WLS inverse provides solutions that only slightly intersect the null space or are orthogonal to it in the case that $W = I$. This has the implication, in the present application, of minimizing local thrust loads and steering losses over the volume that $\Gamma_c \in \Omega^\star$.

In the event that the actuator degrees of freedom are aligned with the principal axes of the constraint ellipsoids, a suitable choice for a diagonal weighting matrix is to choose W such that

$$W_i = \begin{bmatrix} \frac{a_{i1}}{\|B_i^1\|} & 0 \\ 0 & \frac{a_{i2}}{\|B_i^2\|} \end{bmatrix} \tag{20}$$

where $W_i \in \mathbb{R}^{2\times 2}$ is the ith diagonal block of W; a_{i1} and a_{i2} are the principal axis lengths of $\mathcal{E}_i$ and B_i^j is the jth column of B_i. The weights are the constraint ellipsoid dimensions normalized by the relative control effectiveness. Pitch–yaw axis prioritization can be achieved by setting to zero the roll elements of B prior to computing Eq. (20). An empirical analysis using numerical optimization can be used to show that this weight matrix yields a good approximation to the maximum-volume (or maximum pitch–yaw authority) parametrization.

As with any linear allocator, if the commanded acceleration exceeds the boundary of the particular AMS, the effector deflections must change direction in order to access a larger subset of the attainable moments. Suppose along some direction l the maximum admissible particular moment has been determined; that is, $P\Gamma_c \in \partial(\Omega)$.

The following theorem holds:

Theorem 2: For each $P\Gamma_c \in \partial(\Omega)$, there exists an $\varepsilon > 0$ such that $(1+\varepsilon)\Gamma_c \in \Phi$ if there exists a transformation R satisfying $BR = B$ such that $(1+\varepsilon)RP\Gamma_c \in \Omega$.

Proof: If $P\Gamma_c \cap \Omega^\circ \neq \varnothing$, let $P\Gamma_c = \Delta_0 + \Delta_s$ where $\Delta_s \in \partial(\Omega)$ and $\Delta_0 \in \Omega^\circ$. Because P is a linear transformation, $(1+\varepsilon)P\Gamma_c = \Delta_0' + \Delta_s + \varepsilon\Delta_s$ where $\Delta_0' \in \Omega^\circ$, $\Delta_s \in \partial(\Omega)$, and $\Delta_s + \varepsilon\Delta_s \in \Omega^e$ for sufficiently small ε. Suppose a transformation R exists such that $R(\Delta_s + \varepsilon\Delta_s) \in \partial(\Omega)$ and $R\Delta_0' \in \Omega^\circ$; thus, $(1+\varepsilon)RP\Gamma_c \in \Omega$. If $BR = B$, then $(1+\varepsilon)BRP\Gamma_c = (1+\varepsilon)\Gamma_c \in \Phi$ because $BRP = I$ and $P\Gamma \in \Omega \to \Gamma \in \Phi$. □

Remark 1: Transformations satisfying $BR = B$ must be of the form $R = I + N_1 + N_2 + \ldots$, where I is the identity and N_i is a projector onto the kernel of B.

Remark 2: Two necessary conditions for the existence of R are that $P\Gamma_c \cap \Omega^\circ$ is nonempty and $\mathrm{span}(B\Delta_0) = n$. If $P\Gamma_c \cap \Omega^\circ = \varnothing$, this implies that the manifolds $\partial(\Omega)$ and $\partial(\Omega^\star)$ coincide at the point $P\Gamma_c$.

The consequence of the stated theorem is as follows: if the generalized inverse P allocates a control $P\Gamma_c$ such that some subset (but not all) of the controls is in the boundary of the admissible set Ω and those controls not in the boundary span the desired objective, then it is possible to find a transformation R that moves $P\Gamma_c$ toward the subspace of unsaturated controls but is invariant with respect to B (i.e., the "rotation" occurs into the kernel of B). This condition is conceptually illustrated in Fig. 3, where Δ_s is embedded in the constraint boundary and Δ_0 is parallel to it.

Using Theorem 2 and given the aforementioned conditions, a suitable transformation R can be determined as follows: suppose $\Delta = P\Gamma_c$ and that Δ exceeds the boundary of the attainable set along one or more dimensions. Let $\Delta = \Delta_s + \alpha$ where $\Delta_s \in \partial(\Omega)$ and thus $\alpha = \Delta - \Delta_s$, the degrees of freedom of Δ not embedded in the boundary. It is possible to augment the Δ with a vector that is invariant with respect to B by projecting α into the kernel of B.

Let ξ_j form a basis for $\mathcal{N}(B)$, $j = 1, 2, \ldots m-n$. A set of constants x_j is sought that minimizes

$$H = \left\| \left(\Delta + \sum_{j=1\ldots n-m} x_j \xi_j\right) - \Delta_s \right\|^2 \tag{21}$$

describing the norm square error between the intersection of the control vector with the boundary $\partial(\Omega)$ and the augmented control vector. Let the matrix N_B consist of columns $\xi_1 \quad \xi_2 \quad \ldots \quad \xi_{m-n}$, and write their linear combination as

$$\sum_{j=1\ldots m-n} x_j \xi_j = N_B x \tag{22}$$

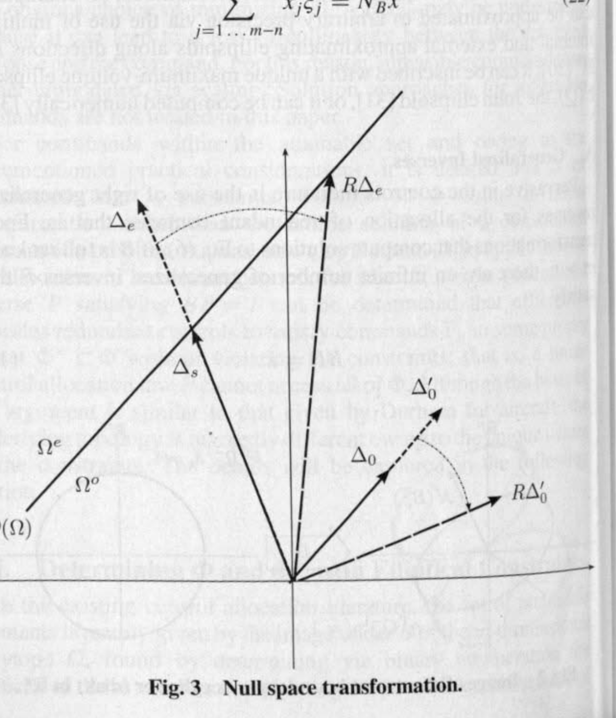

Fig. 3 Null space transformation.

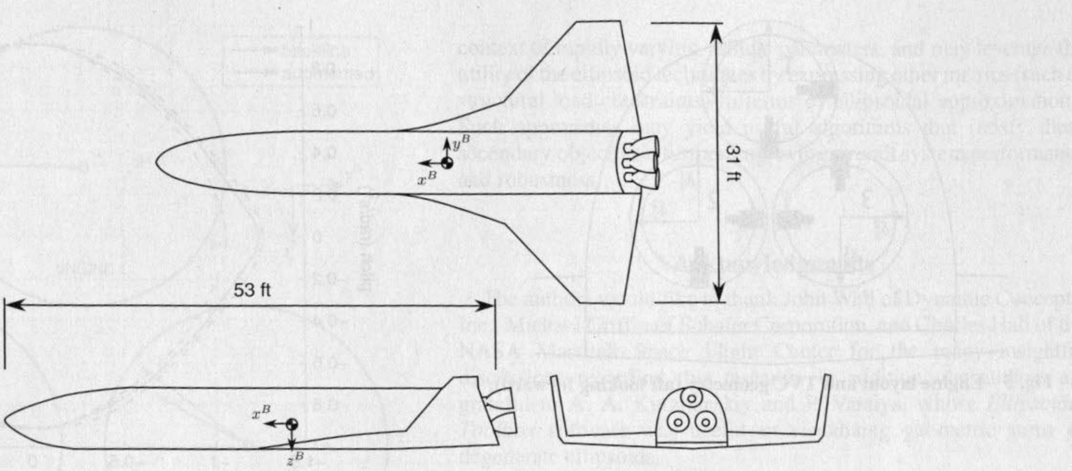

Fig. 4 Concept reusable booster vehicle.

To approximate the solution of

$$N_B x = \Delta_s - \Delta \tag{23}$$

by minimizing Eq. (21), it follows that

$$x = (N_B^T N_B)^{-1} N_B^T (\Delta_s - \Delta) \tag{24}$$

and the augmented control is formed from

$$\tilde{\Delta} = \Delta + N_B (N_B^T N_B)^{-1} N_B^T (\Delta_s - \Delta) \tag{25}$$

Note that $N_B(N_B^T N_B)^{-1} N_B^T$ is an orthogonal projector onto the kernel of B. In the case of symmetric elliptical constraints, the vector Δ_s can be determined directly from the ellipsoids R_i because $\delta_{is} = (\delta_i^T R_i^{-1} \delta_i)^{-(1/2)} \delta_i$.

The analytic constraints enable direct computation of the intersection of Δ with the constraint boundary. It is straightforward to show that the augmented control in Eq. (25) could be rewritten as $\tilde{\Delta} = R\Delta$ so as to satisfy Theorem 2.

A. Practical Considerations

In a practical implementation, the present approach to augmenting the control allocation should be employed only when one or more controls exceeds the saturation boundary; the computation of the saturated control vector Δ_s is trivial to implement. In this scheme, the system retains the linearity properties of the structured generalized inverse over whatever volume of the particular set that inverse has been designed to achieve, while satisfying the secondary metrics of optimality inherent to a least-squares approach; for example, vectoring in a space orthogonal to the null space so as to minimize local parasitic loads on the thrust structure (strictly true only if $W = I$). In the event that one or more actuators is saturated, the augmenting command is computed and applied to access extents of the attainable set not achievable using the generalized inverse alone.

It can be recognized that, in order for the augmented control to be effective, it is necessary that the tangent hyperplane to the constraint boundary associated with the saturated controls have nonzero angle with respect to the null hyperplane. Because the augmentation procedure approximates the solution of the constrained optimization problem by locally projecting the allocation "error" into the null space, the recovered allocation efficiency is less than unity and varies with Γ_c. In the event that the requested moment is infeasible, a secondary computation must be employed to scale the command to lie within the feasible set. Nonetheless, numerical analysis concludes that the efficiency can be substantially increased without requiring iterative computation.

B. Implementation

In a flight software program, the proposed control allocator is implemented as follows:

1) Compute any suitable P satisfying $BP = I$; for example, a WLS allocator.

2) Compute $\Delta = P\Gamma_c$.

3) Compute the scalars $c_i = (\delta_i^T R_i^{-1} \delta_i)^{-(1/2)}$ associated with each thrust vector effector. If no $c_i < 1$, then no augmentation is necessary and $\tilde{\Delta} = \Delta$.

4) If at least one $c_i < 1$, at least one control has saturated. Form the saturated control vector Δ_s from $\theta_{is} = c_i \delta_i$.

5) Compute $\tilde{\Delta} = \Delta + N_B(N_B^T N_B)^{-1} N_B^T (\Delta_s - \Delta)$, where N_B is a basis for the null space of B. In many applications, although B changes substantially due to time-varying mass properties, its kernel N_B remains approximately constant over relatively long intervals. This can be used to the advantage of the implementation by computing N_B offline. The normalization step $(N_B^T N_B)^{-1}$ can be omitted if ξ_j are orthonormal.

V. Example

A numerical example demonstrates the efficacy of the proposed scheme using a nontrivial vehicle model. Consider the reusable booster concept shown in Fig. 4. This vehicle system exhibits several challenging features for thrust vector control allocation due to its asymmetry. To maximize pitch trim control authority at maximum dynamic pressure, the engine thrust plane is negatively canted to align with the nominal center of mass location at this flight condition. In addition, the engines are slightly canted inward to minimize adverse moments due to engine shutdown timing errors. Finally, the

Table 1 Concept vehicle parameters

Parameter	Value
Mass	44650 lbm
Roll moment of inertia J_{xx}	0.2158×10^5 slug · ft^2
Pitch moment of inertia J_{yy}	3.3031×10^5 slug · ft^2
Yaw moment of inertia J_{zz}	3.4301×10^5 slug · ft^2
Cross product of inertia J_{xz}	1.5470×10^3 slug · ft^2
Engine thrust	45000 lbf × 3
Center of mass location (from nose)	$[-30.6500 \quad 0 \quad -2.6400]^T$ ft

Table 2 Concept thrust vector parameters

Parameter	Value
Thrust plane angle	−3.39 deg
Engine gimbal limit	6 deg, circular
Engine 1 gimbal from center of mass	$[-21.21 \quad 0 \quad -2.93]^T$ ft
Engine 2 gimbal from center of mass	$[-21.35 \quad 1.45 \quad -0.43]^T$ ft
Engine 3 gimbal from center of mass	$[-21.35 \quad -1.45 \quad -0.43]^T$ ft

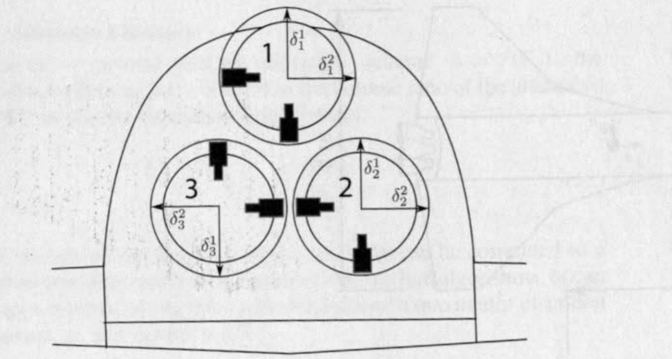

Fig. 5 Engine layout and TVC geometry (aft looking forward).

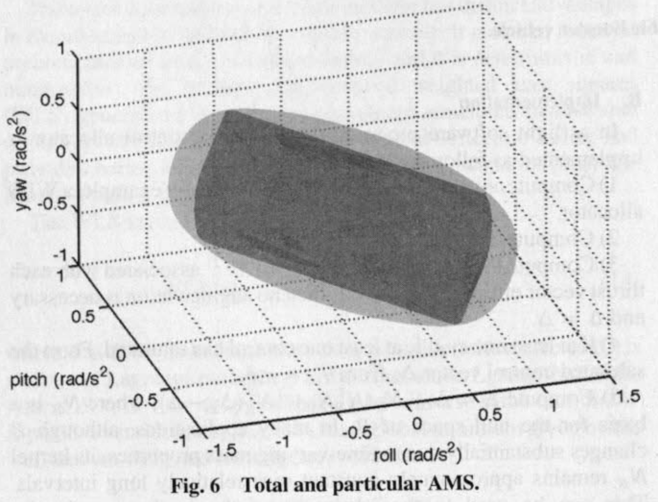

Fig. 6 Total and particular AMS.

presence of wings below the fuselage symmetry plane yields a nondiagonal moment of inertia tensor that couples the instantaneous angular acceleration response to thrust vector inputs.

The general characteristics of the study vehicle at a reference flight condition are given in Table 1. Mass property data are given in a typical aircraft coordinate axis system with the origin at the center of mass.

Engine and thrust vectoring data are given in Table 2. The engine vectoring constraint is assumed to be radially symmetric (circular) with respect to the undeflected (null) position. The engine layout and thrust vector control (TVC) geometry are shown in Fig. 5.

The control effectiveness matrix at this flight condition is

$$B = \begin{bmatrix} -0.0038 & -5.9067 & -3.0139 & -0.6862 & 3.0215 & 0.6862 \\ 2.9171 & -0.0004 & -2.9102 & 0.0039 & -2.9107 & 0.0039 \\ -0.0001 & 2.7561 & -0.0135 & 2.8055 & 0.0137 & -2.8055 \end{bmatrix}$$

and these constraints yield an AMS volume of 3.007 $(\text{rad/s}^2)^3$. Applying Eq. (20) with pitch–yaw axis priority, a suitable weighted least-squares inverse is found to be

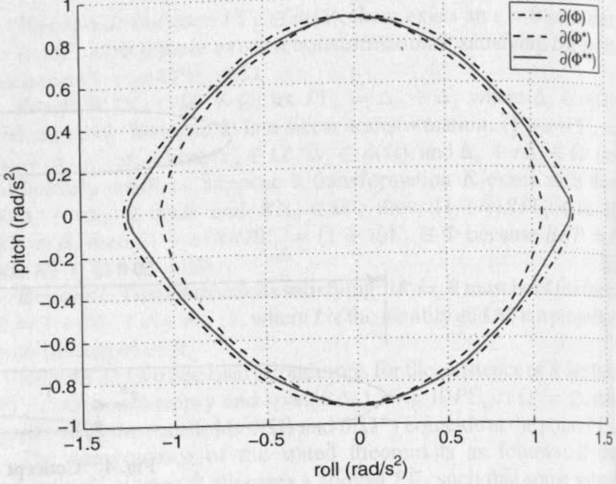

Fig. 7 Pitch–roll AMS projection with augmentation.

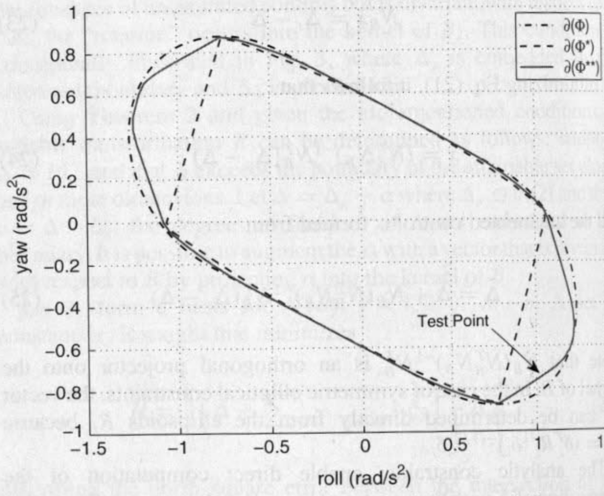

Fig. 8 Yaw–roll AMS projection with augmentation.

$$P = \begin{bmatrix} 0.0000 & 0.1144 & 0.0000 \\ -0.0984 & -0.0001 & 0.0342 \\ -0.0803 & -0.1146 & -0.0701 \\ 0.0480 & 0.0002 & 0.1611 \\ 0.0802 & -0.1143 & 0.0701 \\ -0.0480 & 0.0001 & -0.1611 \end{bmatrix}$$

The three-dimensional shapes of the total AMS and the particular AMS are shown in Fig. 6. The three-dimensional volume accessible using the generalized inverse is depicted in the interior. The volume of the particular set, computed using the gridded bisection method, is

Table 3 Commanded actuator deflections at test point

	Baseline commanded		Augmented commanded	
Actuator	Deflection, deg	Extend (E)/Retract (R)	Deflection, deg	Extend (E)/Retract (R)
Engine 1 pitch	0.000	N/A	0.000	N/A
Engine 1 yaw	7.465	R	5.992	R
Engine 2 pitch	2.022	R	3.297	R
Engine 2 yaw	3.736	R	4.465	R
Engine 3 pitch	2.021	E	3.296	E
Engine 3 yaw	3.736	E	4.466	E

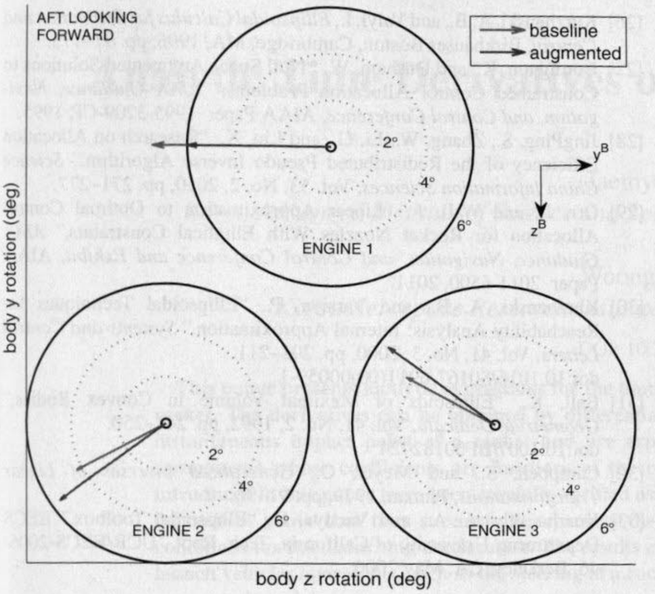

Fig. 9 Nozzle deflection directions at test point.

computed to be 2.033 $(\mathrm{rad}/\mathrm{s}^2)^3$ yielding an allocation efficiency of $\eta = 67.6\%$. Within this volume, command linearity is achieved.

The proposed augmented method is applied to evaluate the increase in allocation efficiency. The result of null command augmentation is shown in Figs. 7 and 8. The three-dimensional AMS has been projected into the pitch–roll and yaw–roll planes, respectively. The boundary of the attainable set using only a generalized inverse is denoted by $\partial(\Phi^{\star})$, and the boundary using the present approach is denoted by $\partial(\Phi^{\star\star})$.

The use of the augmented allocator substantially improves access to the total AMS outside the linear boundary. The efficiency of the augmented allocator is computed to increase to 91.9%, or a volume of 2.764 $(\mathrm{rad}/\mathrm{s}^2)^3$.

The most substantial increase in authority occurs in the lateral-directional maneuvering plane, as seen in Fig. 8. A test point is identified that exists near the boundary of the attainable set for the augmented allocator but outside of the attainable set for the generalized inverse alone. This test point corresponds to the acceleration command of $\Gamma_c = [1.072 \quad 0.000 \quad -0.724]^T$, requiring a simultaneous negative yawing moment near the maximum positive roll angular acceleration. The commanded actuator deflections are given in Table 3 in terms of equivalent degrees of actuator extension or retraction, and the resulting nozzle deflections with respect to the limits are shown in Fig. 9. The control effector positions using only the generalized inverse would fail to achieve the commanded acceleration due to saturation of the engine 1 yaw actuator. The augmented inverse achieves the command while satisfying the constraints.

VI. Conclusions

A hybrid, high-efficiency method of control allocation for complex thrust vector controlled systems has been presented that balances the benefits of the simple structured generalized inverse with the ability to access a substantially larger portion of the attainable set in the event that the control demands exceed the capability of the linear allocation scheme. This method is particularly well suited to vehicles with complex elastic dynamics and servo-inertial coupling whose control design methods, stability analyses, and flight certification processes rely on linearity of the control allocator within the nominal operating envelope.

The present scheme is general in nature, supporting arbitrary vehicle geometry, and scales linearly with the number of effectors. Forward work may seek to extend the present results to time-varying constraint sets so as to consider the dynamic allocation problem in the context of rapidly varying vehicle parameters, and may leverage the utility of the ellipsoid techniques by expressing other metrics (such as structural load constraints) in terms of ellipsoidal approximations. Such approaches may yield useful algorithms that satisfy these secondary objectives, further improving overall system performance and robustness.

Acknowledgments

The authors would like to thank John Wall of Dynamic Concepts, Inc., Michael Griffin of Schafer Corporation, and Charles Hall of the NASA Marshall Space Flight Center for the many insightful discussions regarding this research. In addition, the authors are grateful to A. A. Kurzhanskiy and P. Varaiya, whose *Ellipsoidal Toolbox* software was useful in visualizing geometric sums of degenerate ellipsoids.

References

[1] Enns, D., "Control Allocation Approaches," *AIAA Guidance, Navigation, and Control Conference and Exhibit*, AIAA Paper 1998-4109, 1998.

[2] Bodson, M., "Evaluation of Optimization Methods for Control Allocation," *AIAA Guidance, Navigation, and Control Conference and Exhibit*, AIAA Paper 2001-4223, 2001.

[3] Durham, W., "Constrained Control Allocation," *Journal of Guidance, Control, and Dynamics*, Vol. 16, No. 4, 1993, pp. 717–725. doi:10.2514/3.21072

[4] Durham, W., "Constrained Control Allocation: Three-Moment Problem," *Journal of Guidance, Control, and Dynamics*, Vol. 17, No. 2, 1994, pp. 330–336. doi:10.2514/3.21201

[5] Durham, W., "Attainable Moments for the Constrained Control Allocation Problem," *Journal of Guidance, Control, and Dynamics*, Vol. 17, No. 6, 1994, pp. 1371–1373. doi:10.2514/3.21360

[6] Durham, W., Bolling, J., and Hann, C., "Simulator Implementation of Direct Control Allocation Methods," *AIAA Flight Simulation Technologies Conference*, AIAA Paper 1995-3380-CP, 1995.

[7] Durham, W., "Efficient, Near-Optimal Control Allocation," *Journal of Guidance, Control, and Dynamics*, Vol. 22, No. 2, 1998, pp. 369–372. doi:10.2514/2.4390

[8] Durham, W., "Computationally Efficient Control Allocation," *Journal of Guidance, Control, and Dynamics*, Vol. 24, No. 3, 2001, pp. 521–524. doi:10.2514/2.4741

[9] Bordignon, K., "Constrained Control Allocation for Systems with Redundant Control Effectors," Ph.D. Thesis, Virginia Polytechnic Institute and State University, Blacksburg, VA, 1996.

[10] Bodson, M., and Frost, S., "Control Allocation with Load Balancing," *AIAA Guidance, Navigation, and Control Conference*, AIAA Paper 2009-6270, 2009.

[11] Frost, S., Taylor, B., Jutte, C., Burken, J., Trinh, K., and Bodson, M., "A Framework for Optimal Control Allocation with Structural Load Constraints," *AIAA Guidance, Navigation, and Control Conference*, AIAA Paper 2010-8112, 2010.

[12] Beck, R., "Application of Control Allocation Methods to Linear Systems with Four or More Objectives," Ph.D. Thesis, Virginia Polytechnic Institute and State University, Blacksburg, VA, 2002.

[13] Bolling, J., "Implementation of Constrained Control Allocation Techniques Using an Aerodynamic Model of an F-15 Aircraft," M.S. Thesis, Virginia Polytechnic Institute and State University, Blacksburg, VA, 1997.

[14] Petersen, J., and Bodson, M., "Fast Control Allocation Using Spherical Coordinates," *AIAA Guidance, Navigation, and Control Conference*, AIAA Paper 1999-4215, 1999.

[15] Härkegård, O., "Dynamic Control Allocation Using Constrained Quadratic Programming," *Journal of Guidance, Control, and Dynamics*, Vol. 27, No. 6, 2004, pp. 1028–1034. doi:10.2514/1.11607

[16] Shengyong, T., Shijie, Z., and Yulin, Z., "A Modified Direct Allocation Algorithm with Application to Redundant Actuators," *Chinese Journal of Aeronautics*, Vol. 24, No. 3, 2011, pp. 299–308. doi:10.1016/S1000-9361(11)60035-6

[17] Bolender, M., and Doman, D., "Non-Linear Control Allocation Using Piecewise Linear Functions," *AIAA Guidance, Navigation, and Control Conference and Exhibit*, AIAA Paper 2003-5357, 2003.

[18] Bolender, M., and Doman, D., "Method for Determination of Nonlinear Attainable Moment Sets," *Journal of Guidance, Control, and Dynamics*, Vol. 27, No. 5, 2004, pp. 907–914. doi:10.2514/1.9548

[19] Oppenheimer, M., and Doman, D., "Methods for Compensating for Control Allocator and Actuator Interactions," *Journal of Guidance, Control, and Dynamics*, Vol. 27, No. 5, 2004, pp. 922–927. doi:10.2514/1.7004

[20] Davidson, J., Lallman, F., and Bundick, W., "Integrated Reconfigurable Control Allocation," *AIAA Guidance, Navigation, and Control Conference and Exhibit*, AIAA Paper 2001-4083, 2001.

[21] Demenkov, M., "Reconfigurable Linear Control Allocation via Generalized Bisection," *AIAA Guidance, Navigation, and Control Conference and Exhibit*, AIAA Paper 2005-6341, 2005.

[22] Noll, R. B., and Zvara, J., "Structural Interaction with Control Systems," NASA, Tech. Rept. SP-8079, 1971.

[23] Orr, J., Johnson, M., Wetherbee, J., and McDuffie, J., "State Space Implementation of Linear Perturbation Dynamics Equations for Flexible Launch Vehicles," *AIAA Guidance, Navigation, and Control Conference and Exhibit*, AIAA Paper 2009-5962, 2009.

[24] Orr, J., "A Flight Dynamics Model for a Multi-Actuated Flexible Rocket Vehicle," *AIAA Atmospheric Flight Mechanics Conference*, AIAA Paper 2011-6563, 2011.

[25] Rockefellar, R., *Convex Analysis*, Princeton Univ. Press, Princeton, NJ, 1996, pp. 16–40.

[26] Kurzhanski, A. B., and Valyi, I., *Ellipsoidal Calculus for Estimation and Control*, Birkhauser Boston, Cambridge, MA, 1996, pp. 91–175.

[27] Bordignon, K., and Durham, W., "Null Space Augmented Solutions to Constrained Control Allocation Problems," *AIAA Guidance, Navigation, and Control Conference*, AIAA Paper 1995-3209-CP, 1995.

[28] JingPing, S., Zhang, W., Li, G., and Liu, X., "Research on Allocation Efficiency of the Redistributed Pseudo Inverse Algorithm," *Science China Information Sciences*, Vol. 53, No. 2, 2010, pp. 271–277.

[29] Orr, J., and Wall, J., "Linear Approximation to Optimal Control Allocation for Rocket Nozzles With Elliptical Constraints," *AIAA Guidance, Navigation, and Control Conference and Exhibit*, AIAA Paper 2011-6500, 2011.

[30] Kurzhanski, A. B., and Varaiya, P., "Ellipsoidal Techniques for Reachability Analysis: Internal Approximation," *Systems and Control Letters*, Vol. 41, No. 3, 2000, pp. 201–211. doi:10.1016/S0167-6911(00)00059-1

[31] Ball, K., "Ellipsoids of Maximal Volume in Convex Bodies," *Geometriae Dedicata*, Vol. 41, No. 2, 1992, pp. 241–250. doi:10.1007/BF00182424

[32] Campbell, S., and Meyer, C., *Generalized Inverses of Linear Transformations*, Pitman, 1979, pp. 91–96.

[33] Kurzhanskiy, A. A., and Varaiya, P., "Ellipsoidal Toolbox," EECS Department, University of California, Tech. Rept. UCB/EECS-2006-46, Berkeley, CA, May 2006.